Physics Letters A 372 (2008) 6742–6749

Contents lists available at ScienceDirect

Physics Letters A

www.elsevier.com/locate/pla

Brachistochrones in potential flow and the connection to Darwin's theorem

Roberto Camassa *, Richard M. McLaughlin *, Matthew N.J. Moore, Ashwin Vaidya

Department of Mathematics, University of North Carolina, Chapel Hill, NC 27599, USA

ARTICLE INFO

Article history:
Received 19 February 2008
Received in revised form 12 June 2008
Accepted 13 June 2008
Available online 6 September 2008
Communicated by C.R. Doering

ABSTRACT

We establish the existence and the asymptotic properties of a path of minimum travel time for a line of particles starting upstream of a sphere or cylinder in potential flow. A connection is made between this brachistochrone path and Darwin's proposition which relates the added mass with the drift volume dragged by a body moving an infinite distance in the fluid. We compute an asymptotic correction to the drift volume for finite distances and show how the brachistochrone path is connected to the reflux volume. We present accurate numerical calculations for the brachistochrone position, point of zero horizontal Lagrangian displacement, reflux and partial drift volumes. These calculations are seen to agree well with the asymptotic predictions even for moderate values of the parameters. In the small Reynolds number regimes, we show that while for the case of Stokes flow past a sphere no brachistochrones exist at finite distances from the sphere, the Oseen correction is sufficient to restore such least-time trajectories. Lastly, the application to a sphere falling in a stratified fluid is discussed using the new drift volume correction formula.

The hydrodynamics associated with solid bodies moving in fluids is fundamental in understanding properties of lift, drag, and global energetics. Calculating the fluid flow generally requires integrating the Navier–Stokes equations with boundary conditions at the surface of a solid body moving under hydrodynamic forcing. Because of the complexity of this problem, the intuition regarding the nature of the hydrodynamic forces is often incorrect. Thus, exact mathematical statements regarding such motions are clearly valuable. For example, while aerodynamic lift is correctly understood, it is often incorrectly explained in freshman physics courses by use of Bernoulli's law in which a pressure gradient is inferred by assuming that a particle just above an airfoil will take an equal amount of time to circumvent the body as that of a particle just below the wing. For an interesting discussion of these issues, see the NASA education website [1]. Of course, this equal transit time principle is not justified, and a proper explanation of lift is more complicated (and understood), requiring consideration of the effects of the viscous forces involved.

A somewhat related issue concerns assessing the mass of fluid which is dragged along with a moving body. Of course, this "drift" mass should be expected to depend upon the details of viscous forces involved. Nonetheless there is a general proposition due to Taylor [2] and Darwin [3–8] which predicts the drift mass to be the same as the so-called "added" mass, which for a sphere has been shown to be given by the fluid density times half the volume of the body. Darwin's proposition assumes that the fluid flow is potential and the body has moved an infinite distance through the fluid.

These two problems, that of flight time and transport, are in fact mathematically related, as we show in this Letter. Here we prove the existence of a brachistochrone path for a material planar surface oriented normal to a constant far-field wind advected around a fixed sphere under the assumption of potential flow. This brachistochrone path is defined to be the trajectory of that particle in the upstream plane which crosses a fixed (parallel) downstream plane first. Figuratively, this corresponds to a race from an imaginary starting line to an imaginary finish line drawn in the fluid.

We compute rigorous asymptotics of this path, which allow us to establish the explicit correction formulas for Darwin's drift volume. We work with the two-dimensional case of a cylinder first, and then present the results for the three-dimensional sphere. Shown in Fig. 1 is a schematic detailing the setup of this study. Several of the features in this figure will be described in greater detail below.

The proof of the brachistochrone existence

Consider the problem of computing the time of flight for a plane of particles released a distance d_0 upstream of a cylinder to reach the analogous plane a distance d_0 downstream of the cylinder. For this problem, the stream function is $\psi = Uy(1 - a^2/(x^2 + y^2))$, where a is the cylinder radius and U is the far field flow velocity taken in the x-direction. The time of flight will then be $T = \int_{-d_0}^{d_0} 1/u(x, y)\,dx$. Here u is the horizontal ve-

* Corresponding authors.
E-mail addresses: camassa@email.unc.edu (R. Camassa), rmm@amath.unc.edu (R.M. McLaughlin).

0375-9601/$ – see front matter © 2008 Published by Elsevier B.V.
doi:10.1016/j.physleta.2008.06.093

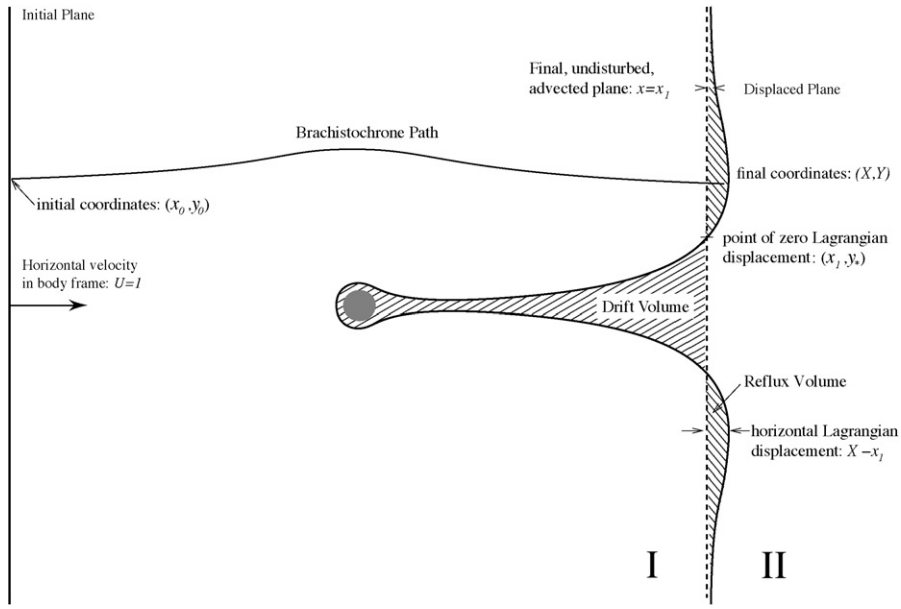

Fig. 1. Schematic depicting the drift and reflux volumes, the point of zero Lagrangian displacement and the brachistochrone path of minimum travel time. Here the figure is drawn in the body frame of reference, and the dashed plane represents the motion of the initial plane were there no sphere present. Equivalently, the dashed plane will be deformed into the displaced plane in the frame of reference in which the fluid is at rest at infinity, and the sphere moves from right to left. The figure has not been drawn to scale to exaggerate certain key features.

locity, $u = \partial_y \psi = U(1 - a^2(x^2 - y^2)/(x^2 + y^2)^2)$, and the curves $(x(t), y(t))$ are level sets of the stream function, $\psi(x, y) = \beta$. We first establish the existence of a brachistochrone path by proving that T has a minimum as function of initial position, $y(0) = y_0$, for fixed $x(0) = -d_0$. By fore-aft symmetry, the time of flight is equal to $T = 2\int_{-d_0}^{0} 1/u(x, y)\,dx$. Note that the horizontal velocity u is always greater than the free stream value U provide $y > x$. Further, the vertical velocity, $v = -\partial_x \psi = -2Ua^2xy/(x^2 + y^2)^2$ is positive for $y > 0$ and $x < 0$. Consequently, $y(t) > x(t)$ provided this holds initially, and provided $x \leqslant 0$. Therefore, u exceeds the free stream value U, for all $-d_0 < x(t) < 0$, and thus the time of flight from $x(t) = -d_0$ to $x(t) = d_0$ is smaller than the free stream time $(= 2d_0/U)$. Lastly, trajectories arbitrarily close to the stagnation line $y(t) = 0$ experience an infinite flight time. By continuity, there must exist a minimum brachistochrone path for this flow. We note that the identical argument extends to the three-dimensional potential flow past a sphere, and also note that for the analogous Stokes low Reynolds number flow past a sphere it can be easily shown that no brachistochrone exists.

The cylinder case

The task of computing the minimum flight time is amenable to rigorous asymptotic analysis. Henceforth, we will non-dimensionalize by introducing coordinates $t' = Ut/a$, and $(x', y') = (x/a, y/a)$, and we will drop the primes. This is equivalent to setting $U = 1$ and $a = 1$ in the formulae above. We will consider the asymptotic limit as the distance from the initial plane to the body grows large, or $d_0 \gg 1$. Numerical evaluation of T in this limit suggest that the minimum flight time occurs for trajectories with initial heights, y_0, growing sublinearly with d_0. It is convenient to study the equivalent limit of large stream values, $\beta \gg 1$, since y_0 is approximately equal to β far from the body.

In order to calculate the time of flight integral explicitly, we seek an approximation of the function $y(x; \beta)$ defined by a streamline. Setting the stream function equal to β gives an implicit formulation for $y(x; \beta)$:

$$y = \beta + \frac{y}{x^2 + y^2}. \tag{1}$$

To obtain an explicit formula for $y(x; \beta)$, we perform Picard iterations on the implicit relation, starting with an initial value $y^0(x) = \beta$. It can be shown that the Picard iteration is convergent for all initial values of $\beta > 1$, which offers a rigorous handle on the control of the order of approximation. Performing the Picard iteration once, gives the following rational approximation to $y(x; \beta)$,

$$y(x; \beta) = \beta + \frac{\beta}{x^2 + \beta^2} + O\left(\frac{\beta}{(x^2 + \beta^2)^2}\right) \quad \text{for } \beta \gg 1, \tag{2}$$

with the error term obtained by performing the iteration once again. We now insert this rational approximation into the horizontal velocity $u = 1 - (x^2 - y^2)/(x^2 + y^2)^2$. Since we are studying large stream function values $\beta \gg 1$, and $y(x; \beta) > \beta$ for all x, the term $(x^2 - y^2)/(x^2 + y^2)^2$ is small and so $1/u$ can be approximated by a geometric series. Retaining terms up to second order in the geometric expansion gives an approximation to the flight time as an integral of a rational function of x and β. The integrals can be evaluated explicitly, and the flight time is approximated by

$$T = 2d_0 - \frac{2d_0}{d_0^2 + \beta^2} + \frac{\arctan(d_0/\beta)}{\beta^3} + O\left(\frac{d_0^5\beta + d_0^3\beta^3 + d_0\beta^5}{\beta^3(d_0^2 + \beta^2)^3}\right) \quad \text{for } \beta \gg 1. \tag{3}$$

The error terms in the approximation of $y(x; \beta)$ and the geometric truncation have been integrated over the same interval to yield the error term shown. The leading order and first correction term in this asymptotic expansion of T are valid for large β $(\beta \gg 1)$ *independent of the magnitude of* d_0. However, the last term retained, $\arctan(d_0/\beta)/\beta^3$, asymptotically dominates the error term if $d_0/\beta \gg 1$, but is of the same order as the error term in other limits. This technicality involving the last term retained (always identifiable by the appearance of an arctan) will also hold in subsequent calculations.

The asymptotic approximation (3) to the flight time can be minimized with respect to β, giving the scaling of the stream value of the brachistochrone path $\beta \sim (3\pi d_0^3/8)^{1/5}$ for $d_0 \gg 1$. For this scaling law, we have $d_0/\beta \gg 1$, which justifies the retention of the highest order term. We note that under these conditions, $y_0 \sim \beta$ and so we have obtained scaling for the initial y-coordinate for

the brachistochrone in the limit of large initial x-coordinate with the error terms being negligible. This scaling has been justified with full mathematical rigor [9], including the subtleties associated with differentiating the asymptotic expansion. We stress that this formula holds only in two dimensions, and a different scaling law will be found in three dimensions. For this special case of two-dimensional potential flow past a cylinder, an exact formula for the flight time is available in terms of elliptic integrals. This formula can be computed quite efficiently using polar coordinates and the exact relations between r and θ provided by the stream function

$$y_\pm = \frac{\beta \pm \sqrt{\beta^2+4}}{2}, \qquad \sin\phi = \sqrt{\frac{r_0^2 - y_+^2}{r_0^2 - y_-^2}}, \qquad k = \frac{y_-}{y_+},$$
$$\frac{T}{2} = y_+\big(F(\phi,k) - E(\phi,k)\big) + r_0 \sin(\phi), \tag{4}$$

where $r_0^2 = d_0^2 + y_0^2$ is the initial radius and F and E are the normal elliptic integrals of the first and second kind, respectively [10]. The asymptotic limits under study here may be obtained directly through Taylor expansions of these elliptic integrals, yielding

$$\frac{T}{2} \sim d_0 - \frac{1}{d_0} + \frac{y_0^2}{d_0^3} + \frac{\pi}{4y_0^3} + O\left(\frac{1}{d_0^2 y_0^3}, \frac{1}{d_0^3}\right), \tag{5}$$

for $d_0 \gg 1$, $y_0 \gg 1$, and $d_0 \gg y_0$, which provides direct confirmation of the asymptotics in Eq. (3). We remark that for the three-dimensional case similar closed form expressions for the flight time involve hyperelliptic integrals, whose direct analysis is somewhat involved, and a direct asymptotic approach on the integrand via Picard iterations is more efficient. We also observe that standard multipole expansions show this scaling law to be universal for general compact bodies in two dimensions, as will the three-dimensional scaling result we compute next.

The sphere case

The same asymptotic Picard iteration-based technique can be adopted for three-dimensional potential flow past a sphere. We take the uniform flow to be in the x-direction and restrict our domain to the plane $z = 0$, so that the three-dimensional radial variable r is given by $r^2 = x^2 + y^2$. The results can afterwards be extended by rotation about the x-axis. The approximation to $y(x;\beta)$, obtained through the stream function $\Psi(r,\theta) = \frac{1}{2}(r^2 - 1/r)\sin^2\theta$, becomes

$$y(x;\beta)^2 = \beta^2 + \frac{\beta^2}{(x^2+\beta^2)^{3/2}} + O\left(\frac{\beta^2}{(x^2+\beta^2)^3}\right) \quad \text{for } \beta \gg 1, \tag{6}$$

where $\beta^2/2$ is the value of the stream function along the level sets $y = y(x;\beta)$, so that we still have the relationship $y(\infty;\beta) = \beta$. The velocity in the plane $z = 0$ is now $(u,v) = (1 - \frac{1}{2}(2x^2 - y^2)/(x^2+y^2)^{5/2}, -\frac{3}{2}xy/(x^2+y^2)^{5/2})$, and $1/u$ is again approximated by a geometric series; however the expression for the flight time is no longer the integral of a rational function—there exist fractional powers in the expression. Nonetheless, further expansion of this expression yields terms which may be integrated explicitly, and the resulting flight time is

$$T \sim 2d_0 - \frac{d_0}{(d_0^2+\beta^2)^{3/2}} + \frac{9\arctan(d_0/\beta)}{32\beta^5} + O\left(\frac{\beta^7 d_0 + \beta^5 d_0^3 + \beta^3 d_0^5 + \beta d_0^7}{\beta^5(\beta^2+d_0^2)^4}\right) \quad \text{for } \beta \gg 1. \tag{7}$$

As before, the last term retained in this asymptotic formula dominates the error term if $d_0/\beta \gg 1$, but is of the same order as the error term in other limits. We will not point out this technicality in subsequent calculations for the sake of brevity. Minimizing the expression with respect to β gives an asymptotic scaling of $\beta \sim (15\pi d_0^4/64)^{1/7}$, a different relation than in two dimensions. Again, under these conditions, $y_0 \sim \beta$, and so the physical height of the brachistochrone path is immediate. We note that this result also follows from a more direct but lengthy asymptotic analysis of the flight time integral with special attention paid to its six branch points [9] (which leads to hyperelliptic integrals), while the present Picard iteration yields a more compact derivation.

Application to Darwin's theorem

An important theorem in hydrodynamics is Darwin's theorem, which relates a quantity know as the 'drift volume' created by a body moving at uniform velocity in an ideal fluid, with the added mass of the body [3]. Here, we define the time-varying 'drift volume' $V_D(t)$ by placing a marked plane of particles perpendicular to the motion of the body and computing the net volume of fluid swept in the same direction as the motion of the object. Fig. 1 depicts a schematic diagram illustrating the key features of this study. The drift volume, as defined in Darwin's theorem, must be taken with the initial and final distances from the plane to the body as infinite (corresponding to a doubly-infinite limit in time) [3]. A subtlety associated with Darwin's theorem is in the ordering of the limits of the size of the plane and the distance of the plane to the body. Eames et al. address this question by taking a disk of particles, with radius ρ_0, at a finite initial distance, x_0, from the body, and allowing the plane to be advected to an infinite distance [4]. Eames et al. compute asymptotic approximations to the drift volume as the initial distance is varied. Here, we derive a generalization of the result of Eames et al., by allowing both the initial and final distances to be finite. These generalized approximations to quantities associated with the drift volume exhibit the desirable property of conservation of volume, in the sense that the volume of material crossing the marked plane always sums to zero, whereas the result of Eames et al. does not exhibit this property [4]. We will recover the formula derived in Eames et al., in the limit as the final distance from the plane to the body becomes infinite, and show precisely where volume conservation is lost. Our fully-finite volume-conserving calculations will be of practical importance in experimental fluid dynamics since only finite times and lengths can be realized in a laboratory setting.

It has been noted that beyond the region in which particles are swept in the same direction as the motion of the body, there lies a region in which the motion of particles is in the opposite direction as that of the body [3,4]. This region is termed the 'reflux region' and the volume swept out by particles moving in the opposite direction as the body is the 'reflux volume'. Here we will present a simple argument, based on conservation of volume, which relates the quantities drift volume, reflux volume, and the volume of the body. We will work in the reference frame in which the fluid is at rest at infinity and the sphere is moving from right to left. In Fig. 1, we divide the domain into two half-spaces: The region to the left of the dashed plane is denoted region I and to the right is region II, where, for this discussion, the figure is interpreted in the reference frame in which the sphere is moving from right to left. For all time, the volume that has entered region I must equal the volume that has exited region I (same for region II). Thus before the body has exited region II, the reflux volume must equal the drift volume, and, after it has exited, the reflux volume must equal the sum of the drift volume and the volume of the body. This argument easily applies to the case of a body moving uniformly in a bounded domain. Note however that this argument holds if the size of the domain is arbitrarily large, provided the flow velocities induced by the motion of the body decay sufficiently fast at infinity. Hence the argument may be extended to free-space po-

tential flow. This volume conservation discussion is summarized in the simple relation

$$V_R = V_D + \bar{V}_S \tag{8}$$

where V_R is the time-varying reflux volume, V_D is the time-varying drift volume and $\bar{V}_S$ denotes the portion of the sphere volume which has crossed the marked Lagrangian plane. Notice that this conservation of volume does not hold for Stokes flow because of the velocity's slow decay at infinity.

The formula for the time of flight (7), can be generalized to give the time it takes a particle on the streamline given by β with initial x-coordinate x_0 to reach an arbitrary final position on the streamline with x-coordinate X,

$$T \sim X - x_0 - \frac{1}{2}\left(\frac{X}{(X^2+\beta^2)^{3/2}} - \frac{x_0}{(x_0^2+\beta^2)^{3/2}}\right) + \frac{9}{64\beta^5}\left(\arctan\frac{X}{\beta} - \arctan\frac{x_0}{\beta}\right) \quad \text{for } \beta \gg 1. \tag{9}$$

This asymptotic relationship gives the final x-coordinate of a particle, X, as an implicit function of the other variables. We will set $T = T_1 \equiv x_1 - x_0$, the time it takes a particle to travel from x_0 to x_1 in the absence of the sphere, and once more invoke a Picard iteration with an initial value $X^0 = x_1$, to obtain the final position of the particle as an approximate, but explicit, function of x_0, x_1, and β,

$$X \sim x_1 + \frac{1}{2}\left(\frac{x_1}{(x_1^2+\beta^2)^{3/2}} - \frac{x_0}{(x_0^2+\beta^2)^{3/2}}\right) - \frac{9}{64\beta^5}\left(\arctan\frac{x_1}{\beta} - \arctan\frac{x_0}{\beta}\right) \quad \text{for } \beta \gg 1. \tag{10}$$

For parameters x_0 and x_1, the volume of the (cylindrically symmetric) reflux region may be given for all times by using Stokes theorem for volumes as $V_R(x_0,x_1) = 2\pi \int_{y_{0_*}(x_0,x_1)}^{\infty} (\tilde{X}(x_0,y_0,T_1) - x_1)\tilde{Y}(x_0,y_0,T_1)\frac{\partial \tilde{Y}}{\partial y_0}\,dy_0$, where $(x_0,y_0) \to (\tilde{X}(x_0,y_0,t), \tilde{Y}(x_0,y_0,t))$ denotes the characteristic map (the solution of the fluid particle ODE's $(\dot{x},\dot{y}) = (u(x,y), v(x,y))$), which yields the marked and deformed Lagrangian plane at any given time t. Here $y_{0_*}(x_0,x_1)$ is the pre-image of the point of zero (horizontal) Lagrangian displacement, so-called because it is the point at which there is no horizontal displacement from the undisturbed advected plane. This special point on the marked plane divides the reflux region from the drift region. By using streamlines, the reflux volume becomes

$$V_R(x_0,x_1) = 2\pi \int_{\beta_*(x_0,x_1)}^{\infty} \big(X(x_0,x_1,\beta) - x_1\big) Y(x_0,x_1,\beta)\frac{\partial Y}{\partial \beta}\,d\beta, \tag{11}$$

where $(X(x_0,x_1,\beta), Y(x_0,x_1,\beta))$ is the stream function map defined as $X(x_0,x_1,\beta) \equiv \tilde{X}(x_0,y(x_0;\beta),T_1)$, $Y(x_0,x_1,\beta) \equiv \tilde{Y}(x_0,y(x_0;\beta),T_1)$. Note that the asymptotics for $\beta \gg 1$ of $X(x_0,x_1,\beta)$ is precisely that given in (10). (For compactness of notation, we will henceforth suppress the explicit dependence on time, x_0 and x_1 in the reflux volume notation.) The value β_* thus identifies the streamline to which the point of zero Lagrangian displacement belongs at any given time t. Far away from the body, the derivative $\partial_\beta Y$ is asymptotic to unity (and $Y(x_0,x_1,\beta) \sim \beta$) and the associated asymptotic corrections have been shown to be subdominant to the corrections dealt with here [9]. The value β_* can be computed by setting the flight time equal to T_1 and $X = x_1$ in (9). Using an approximation for x_0 large and negative, and x_1 large and positive, gives $\beta_* \sim (\frac{9\pi}{32}x_1^2x_0^2/(x_1^2+x_0^2))^{1/5}$. Again, note that under these conditions the asymptotic equivalence between y_0 and β provides the scaling of the physical coordinates for this distinct point. Also observe that under the limit of $x_1 \to \infty$ this yields precisely the same formula for the point of zero horizontal Lagrangian displacement as derived by Eames et al. [4].

The terms in (10) can be integrated explicitly to give an expression for the reflux volume to be evaluated at β_* (higher order terms given by integration have been discarded),

$$\frac{V_R}{V_S} \sim \frac{3}{4}\left(\frac{x_1}{\sqrt{x_1^2+{\beta_*}^2}} - \frac{x_0}{\sqrt{x_0^2+{\beta_*}^2}}\right) - \frac{9}{128{\beta_*}^3}\left(\arctan\frac{x_1}{\beta_*} - \arctan\frac{x_0}{\beta_*}\right) \quad \text{for } x_0 \ll -1,\ x_1 \gg 1. \tag{12}$$

Here the normalization constant, $V_S = 4\pi/3$, is the volume of the sphere. Evaluating at the approximate β_* shown above and expanding in powers of x_0 and x_1 gives a compact approximation to the reflux volume,

$$\frac{V_R}{V_S} \sim \frac{3}{2} - \frac{5}{8}\left(\frac{9\pi}{32}\right)^{2/5}\left(\frac{x_0^2+x_1^2}{x_0^2x_1^2}\right)^{3/5} \quad \text{for } x_0 \ll -1, \text{ and } x_1 \gg 1. \tag{13}$$

The leading order term of this asymptotic expansion is consistent with Darwin's theorem and conservation of volume. By conservation of volume (8), the reflux volume is equal to the sum of the drift volume and the sphere volume if $x_0 < -1$ and $x_1 > 1$. In the case of the sphere, Darwin has established that the drift volume limits to half the volume of the sphere [3] as $x_0 \to -\infty$ and $x_1 \to \infty$. Thus, the reflux volume must approach 3/2 the volume of the sphere in this limit, and this is seen directly in Eq. (13). Finally, we can easily obtain an asymptotic formula for the time-varying drift volume by simply subtracting the volume of the sphere from (13), and this formula gives independent verification of Darwin's calculation for the limiting value of the drift volume, i.e., half the volume of the sphere.

To understand where the conservation of volume principle may be lost, one may transform Eq. (2.10) of Eames et al. [4] into Cartesian coordinates and compare the result to the asymptotic formula for the horizontal displacement (10). Formula (2.10) [4] lacks the second term on the right-hand side of the asymptotic relation (10), $x_1/(x_1+\beta^2)^{3/2}$, because in Eames et al.'s semi-infinite formulation x_1 is taken to infinity a priori. If we take the limit as $x_1 \to \infty$ in formula (10), this term indeed converges to zero. However, the integral of this term over β, as used in the definition of the reflux volume, does not converge to zero but rather to the constant π. This constant represents exactly the amount missing from the reflux volume in order for the conservation of volume formula (8) to hold, in the situation in which $x_1 \to \infty$ prior to integration, i.e., the semi-infinite perspective of Eames et al.

Finally, the conservation of volume formula allows us to compute the quantity called "partial drift volume" introduced by Eames et al. [4], which brings in a cut-off for the volume integral. Geometrically, for as long as the deformed Lagrangian plane can be described by a graph $x(y)$, this corresponds to the volume obtained by integrating over a finite disk of radius $y_{\max}$, $D_P = -2\pi \int_0^{y_{\max}} (x(y) - x_1)y\,dy - \bar{V}_S$. (We have taken an overall minus sign here because we are working in the body frame.) Note that the partial drift volume is not necessarily a physical volume due to the fact that $x(y)$ may change sign. If the radius of the circular plane, $y_{\max}$, is greater than the point of zero Lagrangian displacement then the partial drift volume is the difference between the drift volume and the portion of the reflux volume spanned by the circular plane (and so the partial drift volume may even be negative). By the conservation of volume formula (8), and by using the earlier stream function map notation, the partial drift volume

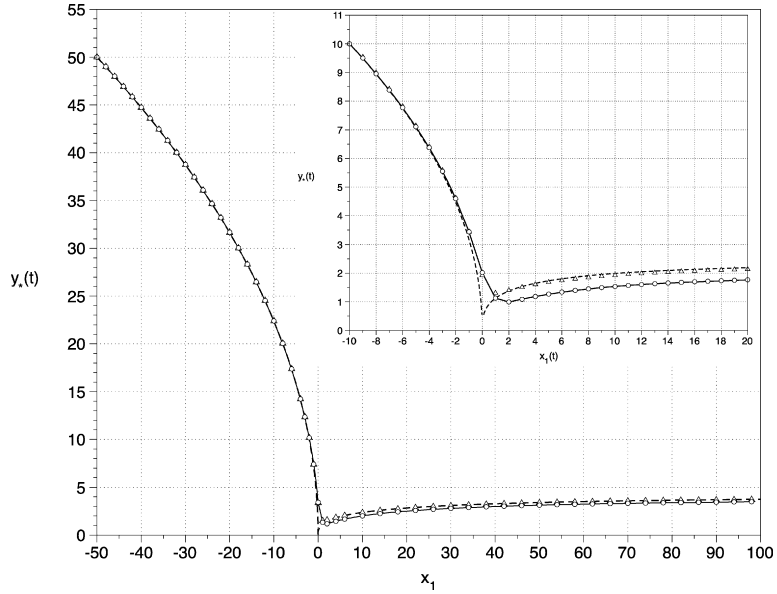

Fig. 2. Point of zero horizontal Lagrangian displacement versus x_1 for the two-dimensional (cylinder) case, with $x_0 = -50$, computed using the Runge–Kutta simulation (circles), asymptotic scalings (dashed line), a numerical root find of the asymptotic formula for the time of flight (triangles), and a similar numerical root find of the exact flight time in terms of elliptic integrals (solid line). The inset shows a blow-up of the region near the origin where the differences among these four methods are most discernible.

may also be written as $D_P = 2\pi \int_{\beta_{\max}}^{\infty} (X(\beta) - x_1) Y(\beta) \partial_\beta Y \, d\beta - \bar{V}_S$, where $\beta_{\max}$ is the streamline parameter corresponding to $y_{\max}$. For $y_{\max}$ sufficiently large, the approximation to the horizontal displacement given in Eq. (10) is uniformly valid over the domain of integration, and so we can readily obtain an asymptotic formula for the partial drift volume,

$$\frac{D_P}{V_S} \sim -\frac{\bar{V}_S}{V_S} + \frac{3}{4}\left(\frac{x_1}{\sqrt{x_1^2 + y_{\max}^2}} - \frac{x_0}{\sqrt{x_0^2 + y_{\max}^2}}\right) - \frac{9}{128 y_{\max}^3}\left(\arctan\frac{x_1}{y_{\max}} - \arctan\frac{x_0}{y_{\max}}\right), \quad y_{\max} \gg 1, \quad (14)$$

where in the body frame, $\bar{V}_S = \frac{\pi}{3}(x_1+1)^2(2-x_1)$ for $x_1 \in [-1, 1]$, $\bar{V}_S = 0$ for $x_1 < -1$, and $\bar{V}_S = 4\pi/3$ otherwise.

We observe that the partial drift formula used in Eames et al. [4] is (in our notation) $D_P^E \equiv -2\pi \int_0^{y_{\max}} \lim_{x_1\to\infty}(\tilde{X}(x_0, y_0, T_1) - x_1) y_0 \, dy_0$. Notice that this definition is approximately the volume between the initial and final position of the marked plane under the asymptotic assumptions considered in Eames et al. [4]. However it is not exact because fluid particles exhibit y-displacements. The combination of $\partial_\beta Y$ in the measure $d\beta$ and the subtraction of the sphere's volume $\bar{V}_S$ accounts for these y-displacements in our theory.

We further remark that we have noticed a formalism by which the semi-infinite theory of Eames et al. [4] may be used to develop finite time corrections, by using asymptotics for different Lagrangian planes and combining them appropriately by appealing to time reversal of potential flow. However the exact details of this procedure are not immediately clear because of the difference between an initially deformed vs. flat plane, and we have not been able to justify this point of view beyond observing that it produces some of the lower order asymptotic terms in our formulation.

Comparison of asymptotics with numerics

Here we present a comparison between our asymptotic formulae and numerical calculations. We see strong agreement between the asymptotics and numerics for all quantities, such as the point of zero Lagrangian displacement, the position of the brachistochrone, and reflux and partial drift volumes in two and three dimensions. For the numerical calculations, we introduce the following flux formulation which provides a highly accurate and efficient method for volume computation. Throughout this discussion, we use the reference frame in which the fluid is at rest at infinity and the body undergoes uniform motion (from right to left), so that velocities are time-dependent: $u(x, y, t) = -\frac{1}{2}(2(x+t)^2 - y^2)/((x+t)^2 + y^2)^{5/2}$, $v(x, y, t) = -\frac{3}{2}(x+t)y/((x+t)^2 + y^2)^{5/2}$. Elementary flux balance arguments show that the time derivative of the reflux volume satisfies the following ordinary differential equation:

$$\frac{dV_R}{dt} = \int_{y_*(t)}^{\infty} u(x_0, y, t)\, dy, \quad V_R(t=0) = 0, \quad (15)$$

where $y_*(t)$ is the point of zero Lagrangian displacement. This point can be tracked through a numerical evaluation of the underlying particle trajectories. Notice that generically this point initially lies at a zero of the horizontal fluid velocity (for the case of the sphere, $y_*(0) = \sqrt{2}|x_0|$). Closed form expressions for the integral in Eq. (15) are available by elementary quadratures, and therefore the only approximation made here is in the numerical tracking of $y_*(t)$. We can compute partial drift volumes through the same methodology, provided we track a different point. The partial drift volume, D_P will satisfy:

$$\frac{dD_P}{dt} = \int_{y_{\max}}^{\infty} u(x_0, y, t)\, dy + \int_{x_0}^{x_*(t)} v(x, y_{\max}, t)\, dx - \frac{d\bar{V}_S}{dt}, \quad D_P(t=0) = 0. \quad (16)$$

Here $x_*(t)$ labels the x-coordinate of the particle whose y-coordinate at time t equals $y_{\max}$. The point $x_*(t)$ may be tracked numerically in a similar fashion as the point of zero horizontal Lagrangian displacement $y_*(t)$. As before, $\bar{V}_S$ denotes the (positive) volume of the portion of the sphere which has crossed the marked Lagrangian plane.

In Fig. 2, we show a study of the point of zero Lagrangian displacement in the two-dimensional case. We compare the numerically tracked position using a fourth order Runge–Kutta simulation

Table 1
Various formulae and scaling laws, asterisks denote entries too long to list in table, ϕ_j correspond to x_j as in Eq. (4). In all columns x_0 is taken as a large negative number.

	2D		3D	
Interval	(x_0, x_1) $x_1 \ll -1$	(x_0, x_1) $x_1 \gg 1$	(x_0, x_1) $x_1 \ll -1$	(x_0, x_1) $x_1 \gg 1$
Brachistochrone streamline parameter	$\sqrt{\frac{x_0^2\lvert x_1\rvert^{1/2}-x_1^2\lvert x_0\rvert^{1/2}}{\lvert x_0\rvert^{1/2}-\lvert x_1\rvert^{1/2}}}$	$(\frac{3\pi}{4}\,\frac{x_0^3x_1^3}{x_0^3-x_1^3})^{1/5}$	$\sqrt{\frac{x_0^2\lvert x_1\rvert^{2/5}-x_1^2\lvert x_0\rvert^{2/5}}{\lvert x_0\rvert^{2/5}-\lvert x_1\rvert^{2/5}}}$	$(\frac{15\pi}{32}\,\frac{x_0^4x_1^4}{x_0^4+x_1^4})^{1/7}$
Zero displacement streamline parameter	$\sqrt{x_0x_1}$	$(\frac{\pi}{2}\,\frac{x_0x_1}{x_0-x_1})^{1/3}$	$(x_0x_1)^{1/3}\sqrt{\lvert x_0\rvert^{2/3}+\lvert x_1\rvert^{2/3}}$	$(\frac{9\pi}{32}\,\frac{x_1^2x_0^2}{x_1^2+x_0^2})^{1/5}$
Reflux volume V_R/V_S	*	$2-\frac{3}{2}(\frac{2}{\pi})^{2/3}(\frac{x_0-x_1}{x_0x_1})^{2/3}$	*	$\frac{3}{2}-\frac{5}{8}(\frac{9\pi}{32})^{2/5}(\frac{x_0^2+x_1^2}{x_0^2x_1^2})^{3/5}$
$T(x_0, x_1)$ asymptotic	$\sum_{j=0}^{1}(-1)^{j+1}\big(x_j-\frac{x_j}{x_j^2+\beta^2}+\frac{\arctan\frac{x_j}{\beta}}{2\beta^3}\big)$		$\sum_{j=0}^{1}(-1)^{j+1}\big(x_j-\frac{x_j}{2(x_j^2+\beta^2)^{3/2}}+\frac{9\arctan\frac{x_j}{\beta}}{64\beta^5}\big)$	
$T(x_0, x_1)$ exact	$\sum_{j=0}^{1}(-1)^j[(E(\phi_j,k)-F(\phi_j,k))y_+-r_j\sin(\phi_j)]$		hyperelliptic integrals	
Added mass	ρV_S		$\rho V_S/2$	

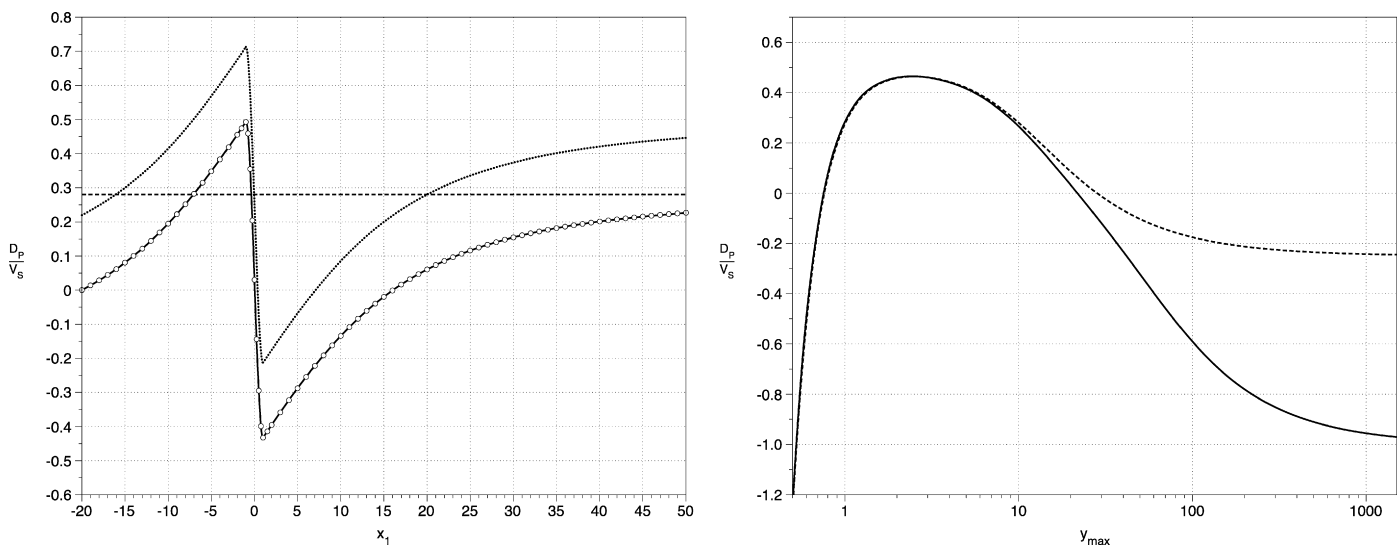

Fig. 3. Comparison of our finite time theory with the semi-infinite formulas (3.5) and (3.9) in Eames et al.'s paper [4] for the three-dimensional case (with $y_{\max}$ corresponding to $\rho_{\max}$). The left panel shows the partial drift volume, normalized by the volume of the sphere, as a function of x_1 with $y_{\max} = 20$ and $x_0 = -20$, as computed using the numerical flux method (shown as dots) and Eq. (14) (the solid line). In the dotted curve Eames et al.'s formula (3.9) is plotted (with x_0 there replaced by our x_1). The dashed line corresponds to taking formula (3.9) of Eames et al. (with x_0 there set to our x_0, here fixed to $x_0 = -20$), and thus gives an asymptote to the solid line (our formula (14) as $x_1 \to \infty$). The right panel shows the partial drift volume as a function of $y_{\max}$, with $x_0 = -10$ and $x_1 = 50$. The solid line shows formula (14) and the dashed line shows the semi-infinite formula of Eames et al. (with x_0 there set to ours). The difference between the horizontal asymptotes as $y_{\max} \to \infty$ of the two curves is accounted for by volume conservation (8) which holds for any finite x_1.

with the asymptotic scaling given in row 4, columns 2 and 3 of Table 1 (where standard matrix entry notation is followed for the row and column labeling). Also shown is the point of zero Lagrangian displacement calculated numerically by setting the flight time equal to $x_1 - x_0$ in the asymptotic formula (row 6, columns 2 and 3 of Table 1), as well as the exact formula involving elliptic integrals (row 7, columns 2 and 3 of Table 1). The figure shows overall excellent agreement between the asymptotic formulae, exact expressions, and numerical simulations. See the caption for details.

In Fig. 3, we present a study of the partial drift volume D_P. We show the asymptotics for D_P given in (14), normalized by the volume of the sphere, plotted first as a function of x_1, and then as a function of the cut-off parameter $y_{\max}$, with x_0 considered as a parameter. We show the comparison to the semi-infinite formulae of Eames et al. [4], which corresponds in our theory to taking one of x_0 or x_1 to infinity a priori. The comparison in Fig. 3(a) shows excellent agreement between the numerically computed values and Eq. (14), as well as substantial differences with the semi-infinite perspective. The parameters here were chosen to replicate possible laboratory parameters. Finally, the depiction in Fig. 3(b) of the partial drift volume as a function of the cut-off parameter, $y_{\max}$, illustrates an important difference between formula (14) and the corresponding semi-infinite formula of Eames et al. [4]. The leading order of formula (14) as $y_{\max} \to \infty$ is consistent with the conservation of volume principle (8). However, the principle of volume conservation (8) is absent when taking $x_1 \to \infty$ *prior* to the volume integration (which corresponds to the semi-infinite theory of Eames et al.). Volume conservation (8) is violated in this case by an amount which may be computed by retaining finite x_1 and calculating the integral contribution to the partial drift volume of a term that converges to zero in the limit as $x_1 \to \infty$ (discussed above). We computed this integral contribution to be π. Normalizing by $V_S = 4\pi/3$ gives 3/4 which accounts precisely for the difference between the two horizontal asymptotes shown in Fig. 3(b).

In Fig. 4, we show the vertical position of the brachistochrone path for the sphere case (three dimensions) along with the reflux volume as x_1 is varied. For the position of the brachistochrone path (Fig. 4(a)) we show the numerical tracking with the fourth order Runge–Kutta simulation versus the asymptotic scalings shown in row 3, columns 4 and 5 of Table 1. The figure shows good agreement apart from the region in which the vertical position of the brachistochrone path becomes small, i.e. where the asymptotic formulae cannot be expected to hold. The reflux volume is shown in Fig. 3(b) as computed by three methods: the flux numerical method, asymptotic equation (13), and Eq. (12) with the point of zero horizontal displacement computed by a numerical root-find of Eq. (9). The figure shows excellent agreement between the

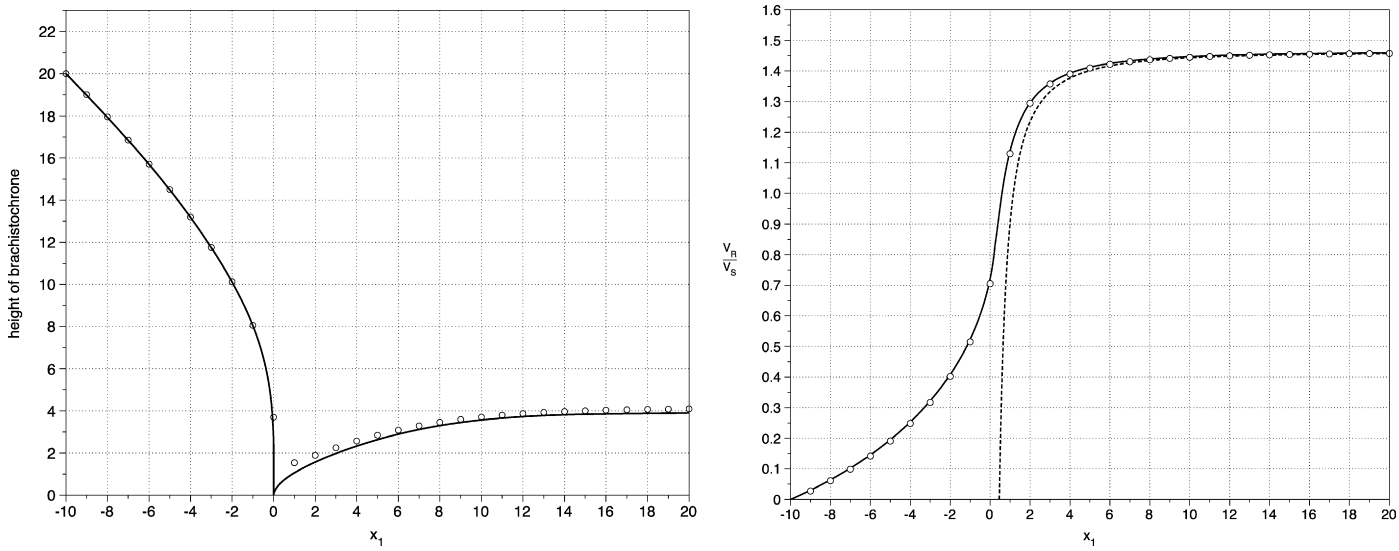

Fig. 4. The left panel shows the vertical position of the brachistochrone path for the three-dimensional (sphere) case as a function of x_1, with $x_0 = -10$. The circles show values given by numerical tracking and the solid line represents the asymptotic scalings. The right panel shows the reflux volume as a function of x_1, with $x_0 = -10$ computed by three methods. The circles show the results of the numerical flux method, the solid line is Eq. (12) with the point of zero Lagrangian displacement computed by a numerical find of Eq. (9), and the dashed line is the asymptotic equation (13).

asymptotic expressions for reflux volume and the numerical flux formulation.

Discussion

These calculations present two new results: first, the existence proof and explicit computation of a universal brachistochrone path for potential flows arising from a single obstacle moving at constant speed; and, second, the explicit calculation of quantities associated with the drift volume, including an asymptotic correction accounting for finite lengths of travel. The present formulation is distinguished from earlier results in that the calculations are done in finite time, whereas prior studies have either concerned the infinite time result [2,3,5–8], or explored the approach to the infinite time limit using semi-infinite time results [4]. We emphasize that volume conservation by which the reflux volume is the sum of the drift volume and the body volume, i.e. Eq. (8), holds throughout our calculations, whereas this conservation principle is lost in the semi-infinite limit approach [4] and is specifically associated with an interchange of limits with an infinite integral. Consequently, the present study offers insight into the subtleties associated with the incommensurate limits observed previously [4].

The new result establishing the asymptotic properties of the brachistochrone path improves the geometric description of the reflux volume. Further, it shows a fundamental difference in the fluid transport properties between Stokes flows and potential flows. Using the same approach as above to establish the mathematical existence of the brachistochrone path for potential flow, it can be shown that no brachistochrone path exists for Stokes flow past a sphere in free space. To appreciate these differences, Fig. 5 documents the evolution of a line of fluid particles under potential, Stokes and Oseen flows past a sphere. The Oseen case from Lamb's approximate stream function [11] is depicted for Reynolds numbers (based on the sphere diameter) 0.5 and 1. The Stokes solution shows no brachistochrone, whereas the Oseen solutions do develop a minimum, though farther from the body (and of smaller magnitude) than its potential counterpart. In this regard, the brachistochrone may be loosely interpreted as a signature of inertia in an infinite fluid system. It is also noteworthy to compare the drift volumes of these three cases: clearly the Stokes case is dragging the most fluid, consistent with the familiar Stokes paradox, while the potential flow draws the least amount.

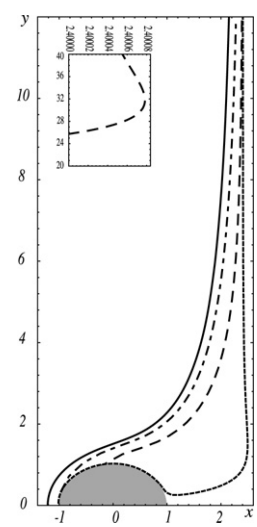

Fig. 5. Evolution of upstream plane flowing past a sphere, with $x_0 = -1.6$, $a = 1$, $t = 4$ under Stokes (solid), Oseen with $Re = 0.5$ (short-long dash), and $Re = 1$ (long dash), respectively, and potential flow (short dash): insets document the emergence of the minimum in the far field Oseen flow, absent in the case of Stokes flow, for $Re = 1$ and $Re = 0.5$, respectively. Note that the Oseen flow satisfies the no-slip boundary condition on the sphere only approximately.

Application to falling sphere in stratified fluid

Lastly, we discuss the application of these formulae to the motion of a sphere falling in a stably stratified miscible fluid system with sharp two layer stratification. Abaid et al. [12] documented in experiments that a sphere which had density greater than the densities of the fluids in such a tank could experience a reversal of motion in which the descending sphere arrested, rose on a short timescale, before ultimately returning to slow descent. A coarse criterion can be drawn from the drift volume using the assumption of potential flow past a sphere, by insisting that for a reversal of motion to occur the net density of the conglomerate

sphere plus drift fluid must necessarily be less than the density of the bottom layer fluid, in order to have negative buoyancy in the system. It is interesting to consider first the prediction of a stopping criterion based upon Darwin's theorem in comparison with those prior measurements. The density of the conglomerate is $(M_d + M_s)/(V_d + V_S)$ where M_d, M_s, V_d, V_S are the respective masses and volumes of the drift fluid and sphere. Let the proportionality factor relating the drift volume to the sphere volume be denoted as c, with $c = 1/2$ in Darwin's case where the sphere travels a doubly infinite distance through the fluid. More generally, c is determined by the corrected finite time asymptotic formula given in Eq. (13). The coarse criterion then becomes $(c\rho_0 + \rho_s)/(1 + c) < \rho_b$ where ρ_b, ρ_s, ρ_0 are the respective densities of the bottom fluid, sphere and top fluid density. It should be stressed that such a criterion is overly coarse in that it does not account for mixing, additional hydrodynamic forces, and the possibility that part of the drift volume shears away. Nonetheless, the arrest criterion based on Darwin's prediction and its finite time counterpart derived here can be checked to assess their quantitative relevance. First, with the fluid densities of $\rho_b = 1.0385g/cc$, $\rho_0 = 0.997g/cc$ used by Abaid et al., the criterion based on Darwin's drift volume $c = 1/2$ predicts that the sphere should arrest if its density is smaller than $1.05925g/cc$, which should be compared with the experimentally determined threshold of $1.045g/cc$ above which the sphere did not arrest. Not surprisingly, the coarse prediction using Darwin's theorem overestimates the maximum density of the sphere that can be stopped by entrained drift volume, yet it does give a first rough estimate of this critical density. This estimate can be improved with the finite time criterion. The sphere radius in the experiments was $a = 0.25$ cm, the sphere was observed to arrest within approximately 5 radii of the transition layer, and the distance traveled to the transition layer was approximately 50 radii. With these parameters, and the corrected drift volume formula, the arrest prediction improves, with the critical density value being $1.05565g/cc$. Note that the deviation between the drift volume asymptotic formula and numerical evaluation for these values of x_0 and x_1 is extremely small (changing this critical density only in the 5th significant digit).

It goes without saying that further study is merited in understanding these complex problems, but the calculations performed here do offer some improved understanding of the transport associated with moving bodies in fluids.

Acknowledgements

R.C. is partially supported by DMS-0509423 and NSF DMS-0620687. R.M.M. is partially supported by NSF DMS-030868, M.N.J.M. is supported by an NSF Collaboration in Mathematical Geosciences (CMG) grant, NSF ATM-0327906, and an NSF Research Training Group (RTG) grant, NSF DMS-0502266, and A.V. is supported by RTG NSF DMS-0502266. We thank Andrea Prosperetti for alerting us to some of the references on Darwin's Theorem and pointing out its connection with the brachistochrone problem.

References

[1] http://www.grc.nasa.gov/WWW/K-12/airplane/bernnew.html.
[2] G.I. Taylor, Proc. R. Soc. London A 120 (1928) 13.
[3] C. Darwin, Proc. Cambridge Philos. Soc. 49 (1953) 342.
[4] I. Eames, S.E. Belcher, J.C.R. Hunt, J. Fluid Mech. 275 (1994) 201.
[5] M.J. Lighthill, J. Fluid Mech. 1 (1956) 31.
[6] C.-S. Yih, J. Fluid Mech. 152 (1985) 163.
[7] C.-S. Yih, J. Fluid Mech. 347 (1997) 1.
[8] T.B. Benjamin, J. Fluid Mech. 169 (1986) 251.
[9] R. Camassa, R.M. McLaughlin, M.N.J. Moore, A. Vaidya, in preparation.
[10] P.F. Byrd, M.D. Friedman, Handbook of Elliptic Integrals for Engineers and Scientists, Springer-Verlag, New York, 1971.
[11] C. Pozrikidis, Introduction to Theoretical and Computational Fluid Dynamics, Oxford Univ. Press, New York, 1997.
[12] N. Abaid, D. Adalsteinsson, A. Agyapong, R.M. McLaughlin, Phys. Fluids 16 (5) (2004) 1567.